Supplementary information for

A Multiplexed Chemical Sensing Imager

Di Wang[1,2,#,*], Fenni Zhang[2,3,#], Kyle R. Mallires[2], Vishal Varun Tipparaju[2], Jingjing Yu[2], Erica Forzani[2], Changku Jia[4,5,*], Nongjian Tao[2], Xiaojun Xian[2,*]

[1]Research Center for Intelligent Sensing, Zhejiang Lab, Hangzhou 311100, China.

[2]Center for Bioelectronics and Biosensors, Biodesign Institute, Arizona State University, Tempe, Arizona 85287, USA.

[3]Biosensor National Special Laboratory, Key Laboratory for Biomedical Engineering of Education Ministry, Department of Biomedical Engineering, Zhejiang University, Hangzhou 310027, PR China.

[4]Department of Hepatobiliary Pancreatic Surgery, Affiliated Hangzhou First People's Hospital, Zhejiang University School of Medicine, Hangzhou 310006, China.

[5]Research Center of Diagnosis and Treatment Technology for Hepatocellular Carcinoma of Zhejiang Province, Hangzhou 310006, China.

*Corresponding author: diwang@zhejianglab.com; jiachk@126.com; xiaojun.xian@asu.edu

#These authors contributed equally to this work

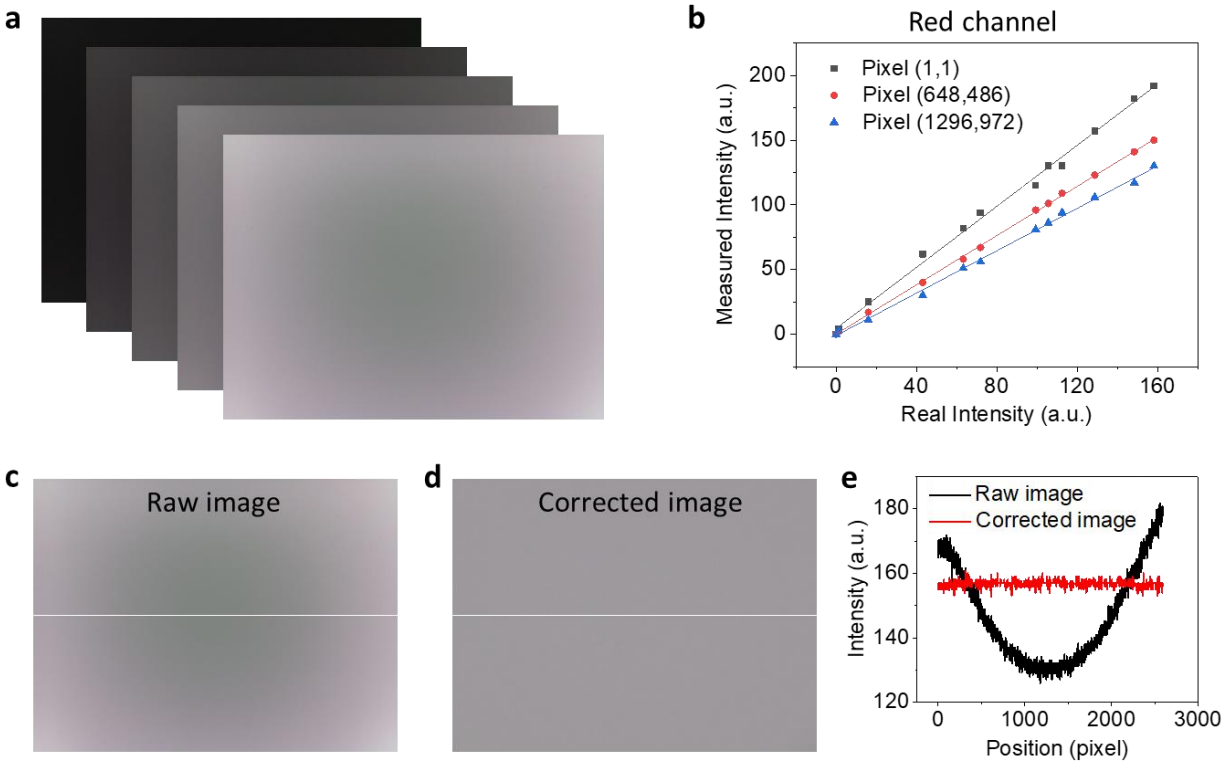

Fig. S1. Calibration of a CMOS imager and flat-field correction of images. a, A sequence of images were captured by CMOS with different illumination intensities. For each image, the averaged intensity of each color channel (R, G and B) over the whole image was set as the "real intensity". **b,** For each pixel, the measured intensity was linearly fitted as a function of "real intensity". Pixels at different locations had significantly different sensitivities. **c,** A raw image captured by CMOS imager. The corners and the center showed different brightness and color tones. **d,** Flat-field corrected image. Each color channel of the raw image was corrected pixel by pixel based on the linear relationship between measured intensity and "real intensity". Then the corrected image was obtained by merging the three corrected color channels. **e,** Intensity plots along the white lines in **c** and **d**. The intensity variation between pixels was greatly reduced after correction.

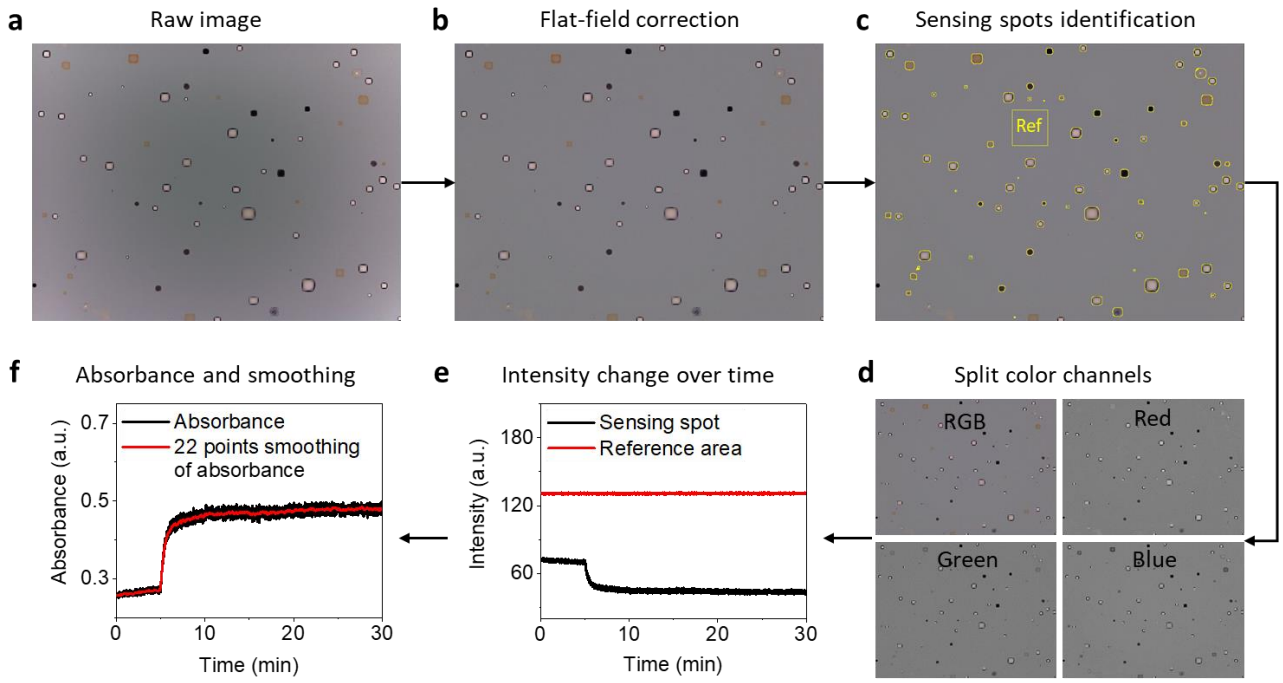

Fig. S2. Data processing: from raw images to absorbance signal. a, A raw image of sensing spots captured by C-CMOS chip. **b,** Flat-field corrected image. **c,** Identification of sensing spots and a blank (reference) area using Image J. **d,** Split of color channels for analyses of different types of sensing spots. **e,** Intensities of a sensing spot (I_{sensor}) and the reference area (I_{ref}) were obtained by analyzing a stack of captured images. **f,** Absorbance signal was calculated with the equation of *absorbance* = -log(I_{sensor}/I_{ref}), then the signal was smoothed using a time window of 15 s (22 frames) to reduce noise.

Table S1. Comparison of C-CMOS and conventional gas detection tubes.

	NO_2	CO_2	NH_3	C_3H_6O
C-CMOS: Detection limit (ppm) [a]/ Sampling time (s)	0.16/15	71/15	0.33/15	445/15
RAE tubes: Detection limit (ppm) / Sampling time (s)	0.5/90	150/240	0.5/180	500/240

a. The calculation of detection limit is based on the calibration curves in main text Fig. 3. To calculate the detection limit, a signal threshold is defined based on the zero concentration responses (mean: $Signal_{zero}$, standard deviation: Std_{zero}) with the equation of $Signal_{threshold} = Signal_{zero} + 3 \times Std_{zero}$. With this signal threshold, the detection limit is obtained by substituting it into the calibration curve. The detection limits can be lower if longer sampling time is used.

Noise Analysis

Read noise and dark noise

Two images were captured under dark condition (same exposure time). A differential image was obtained by calculating the difference between the two images. The standard deviation of the intensities of all the pixels in the differential image was calculated (SD_{Diff}). The read noise (N_{R}) and dark noise (N_{D}) of a N pixels area were calculated by,

$$N_{\mathrm{R}} + N_{\mathrm{D}} = \frac{SD_{\mathrm{Diff}}}{\sqrt{2} \times \sqrt{N}} \quad (1)$$

Shot noise

The full well capacity of the CMOS imager was 4300 e^-, and the corresponding shot noise (N_{S}) scaled with the pixel number (N) as,

$$N_{\mathrm{S}} = \frac{\sqrt{\frac{4300}{256} \times Intensity} \times \frac{256}{4300}}{\sqrt{N}} \quad (2)$$

Light source noise

300 images were captured under normal experimental condition. The average intensity of each image was calculated. The standard deviation of the averaged intensities was used to present light source noise (N_{L}).

Noise of a reference area and a sensing spot

300 images of a reference area and a sensing spot were captured. The sizes of the reference area and the sensing spot were both 2493 pixels, and the standard deviations of their intensity signals were calculated to present their total noise levels. The noise contributed by digital noise, dark noise, shot noise, and light source noise (N_{RDSL}) was calculated by:

$$N_{\mathrm{RDSL}} = \sqrt{(N_{\mathrm{R}} + N_{\mathrm{D}})^2 + {N_{\mathrm{S}}}^2 + {N_{\mathrm{L}}}^2} \quad (3)$$

Table S2 shows the noise components, the total noise of the reference area and the sensing spot. N_{RDSL} contributed to most of the noise of the reference area but contributed to less than half of the noise of the sensing spot. Because images of the reference area and the sensing element were captured under the same condition, the extra noise of the sensing spot was originated from the sensing materials. This

additional random noise component can be reduced by averaging over more pixels (spatially) and more frames (temporally), as shown in Fig. 4b in the main text.

Table S2. Noise components and total noise of a reference area and a sensing spot.

	$N_R + N_D$	N_S	N_L	N_{RDSL}	Total noise
Reference area	0.012	0.059	0.033	0.069	0.084
Sensing spot	0.012	0.046	0.033	0.058	0.147